Ensuring Accurate Fieldline-Body Intersection

Wayne Arter*
with V. Riccardo*, M. Mattei‡and G. Saibene†

Culham Centre for Fusion Energy*
Culham Science Centre, Abingdon, Oxfordshire OX14 3DB, UK
and Universit degli Studi Mediterranea di Reggio Calabria‡
Via Graziella 89100, Reggio Calabria, Italy
and F4E Fusion for Energy†
c/ Josep Pla no 2 Torres Diagonal Litoral Edificio B3
08019 Barcelona, Spain

Work funded by F4E contract F4E-OPE-148, EURATOM, and EPSRC contract EP/E034438/1.

CCFE
CULHAM CENTRE FOR FUSION ENERGY

Outline

MOTIVATION

SMARDDA

FIELD-LINE FOLLOWING

GEOMETRY AND MESH

RESULTS

SUMMARY

ITER tokamak first wall

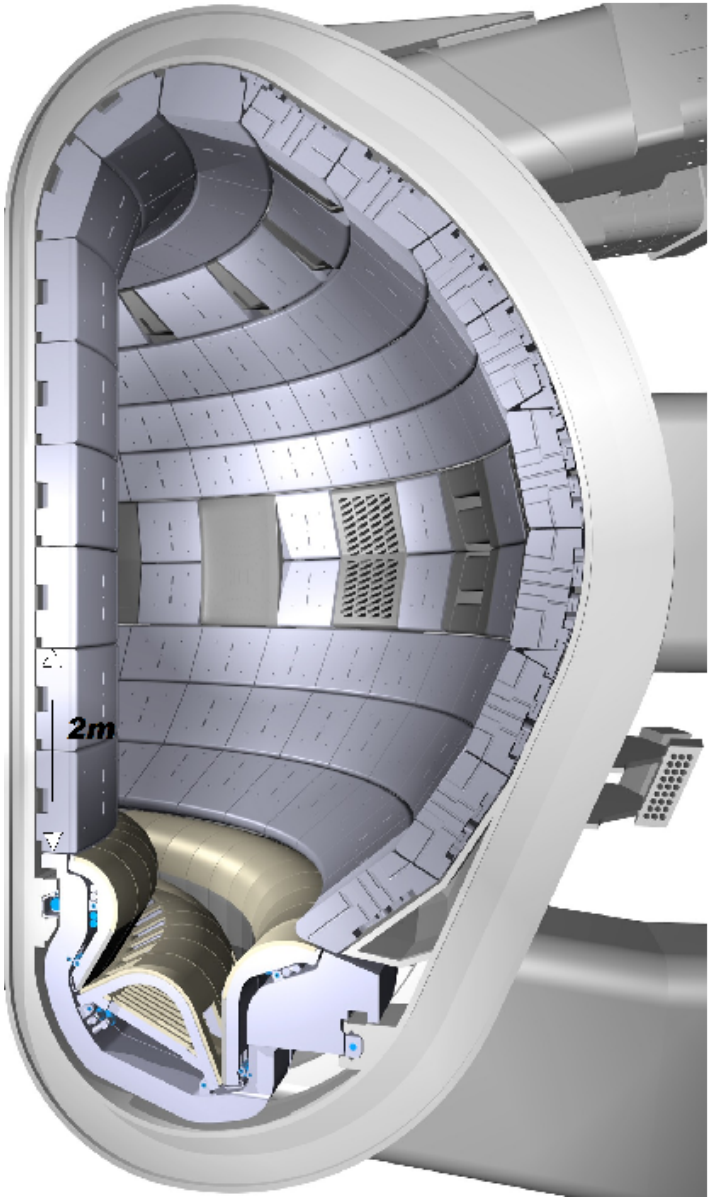

Motivation: estimate Q (heat flux) to ITER first wall, using fitting formula which requires data from field-line following calculation.

- Cut through ITER tokamak showing first wall consisting of ≈ 500 metre square panels.
- Panels designed for mutual protection by neighbours from heat flux directed along field.

CCFE CULHAM CENTRE FOR FUSION ENERGY

Significant Facts

- ψ calculated using either finite element or finite difference methods as part of a time evolution problem. Typically second order accurate.
- On relevant timescales, field-lines are steady.
- Sharp exponential fall-off (typically 50 mm scrape-off length) of heat flux Q with $\psi - \psi_b$, where ψ_b is the highest value of ψ for any part of the silhouette.
- Heat flux proportional to $\mathbf{B}.\hat{\mathbf{n}}$, where $\hat{\mathbf{n}}$ is surface normal.

Equilibrium Calculation

- Poloidal magnetic flux ψ representation of a 6.0 T, 7.3 MA plasma in the ITER tokamak. The dashed line corresponds to the inner edge of the first wall in silhouette.
- Field-lines lie on surfaces of constant ψ. A toroidal field component $f(\psi)$ (not shown) causes field-lines to wrap around the torus in azimuthal angle ζ.
- Convention that ψ is a maximum on the (minor) axis.
- Blue marks the mapped region, discussed later.

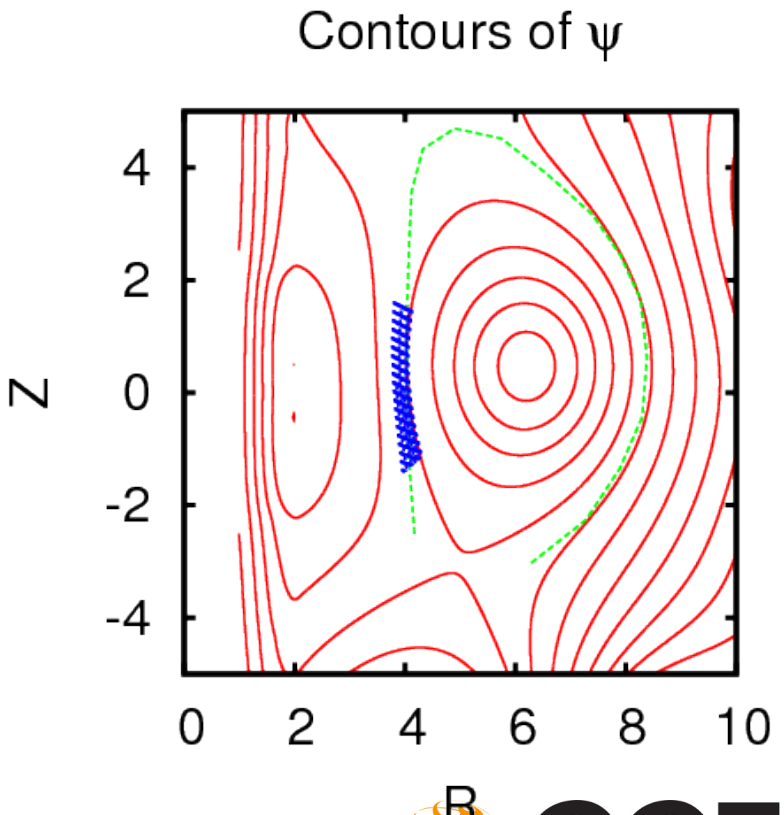

Outline of Solution

- `vtk` file input of triangulated geometry from CATIA (using CADfix package for CAD import/repair/meshing/export).
- Field-line following in special coordinates with specially tailored RK scheme (to be explained).
- Efficient line/particle tracking (by SMARDDA, to be explained).
- Spatial subdivision – octree hierarchical data structure (HDS).
- Efficient track intersection with geometry (after Badouel)

Badouel, Graphics Gems p.390, Academic Press, 1990

SMARDDA = SMART+DDA hybrid

- General design for both neutrals and charged particles, now extended to field-lines tracked with adaptive scheme.
- Octree provides best results for tracking particles over a long distance, whereas regular cuboid lattice (SEADS) works best for fine detail, so use a hybrid approach.
- Domain is split further where there are objects.
- Particles are tracked within and across cells using DDA algorithm (Fujimoto *et al*).

Fujimoto *et al*, IEEE CG & Appl 6,16, 1986

Ray-patch intersection algorithm

Simplified representation of scheme in 2-D:

- Neutral particles shown as straight-lines
- Charged particles as curved trajectories.
- Curved trajectory treated as a series of short straight lines.

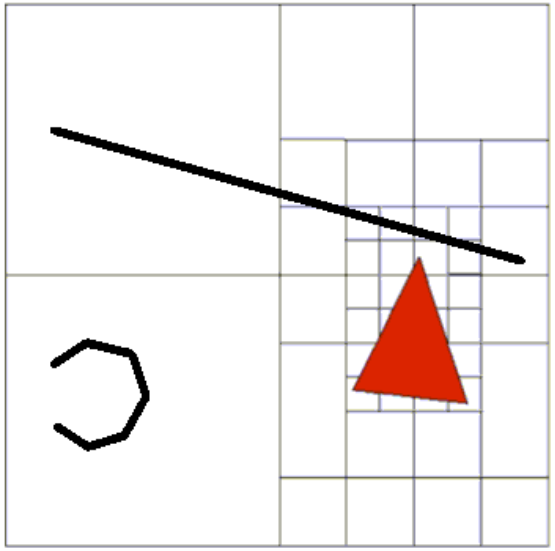

Ray-patch intersection algorithm

- Quick test whether charged particle occupies same cell at start and end of step. Use bit-manipulation with the exclusive-or (IEOR) function (cf. SMART algorithm)
- Two binary vectors $\mathbf{N}^1$ and $\mathbf{N}^2$ occupy the same octree cell cuboid of side $2^{n_{sh}}$ if for every component label $i = 1, 2, 3$

$$\sigma_i = ISHFT(IEOR(N_i^1, N_i^2), -n_{sh}) = 0 \qquad (1)$$

- Example of size $2^4 = 16$ cell in 1-D. The trailing 4 bits are shifted out, then `IEOR` performed on the rest.

$$\begin{aligned} 1 &= 0...00001 \ \text{shift} \ \rightarrow 0...0 \\ 7 &= 0...00111 \ \text{shift} \ \rightarrow 0...0 \\ 17 &= 0...10001 \ \text{shift} \ \rightarrow 0...1 \end{aligned}$$

For 1 and 7, `IEOR` gives a zero indicating the cell is the same, not so 1 and 17.

Spackman & Willis, Computers & Graphics 15,185, 1991

Coordinate System 1

Field-line given parametrically as $\mathbf{x}(t)$ where

$$d\mathbf{x}/dt = \mathbf{B}(\mathbf{x}) \tag{2}$$

- Ideally, choose system where field-lines are straight.
- Very difficult for flux lines near X-point.
- Compromise, use coordinates (ψ, ζ, θ), where

$$\tan\theta = Z'/R' = (Z - Z_c)/(R - R_c) \tag{3}$$

  θ cf. cylindrical polar angle about (R_c, Z_c), define minor radius $r = \sqrt{(R'^2 + Z'^2)}$.
- Field-lines are nearly straight.

Coordinate System 2

Formula in general axisymmetric geometry for field-line in terms of flux function $\psi(x^1, x^2)$:

$$\dot{x}^k = \frac{1}{\sqrt{g}} \left(\frac{\partial \psi}{\partial x^2}, -\frac{\partial \psi}{\partial x^1}, \sqrt{g} B^3 \right) \tag{4}$$

Choose $x^1 = \psi$, $x^2 = \theta$, $x^3 = \zeta$ and use relation $B^3 = -f/R$, field-line equation becomes:

$$\frac{d\theta}{d\zeta} = \frac{1}{f} \cdot \frac{R}{\sqrt{g}} \tag{5}$$

where the inverse Jacobian is

$$\frac{1}{\sqrt{g}} = \left.\frac{\partial \psi}{\partial R}\right|_Z \left.\frac{\partial \theta}{\partial Z}\right|_R - \left.\frac{\partial \psi}{\partial Z}\right|_R \left.\frac{\partial \theta}{\partial R}\right|_Z$$

Runge-Kutta-Fehlberg Method

Second-third order RK method for autonomous system Eq (5)

Butcher array:

$$
\begin{array}{c|ccc}
0 & & & \\
- & 1 & & \\
- & \frac{1}{6} & \frac{1}{3} & \\
\hline
 & \frac{1}{2} & \frac{1}{2} & \\
 & \frac{1}{4} & \frac{1}{4} & \frac{1}{2}
\end{array}
$$

- Simple coefficients, simple geometrical interpretation.
- Step-size control after Shampine & Watts.
- Tests show that accuracy per time-step may be tightly controlled.

Shampine & Watts, Applied Math & Comp 5,93, 1979

Discrete mapping

Evaluation of $R(\psi, \theta)$ and $Z(\psi, \theta)$:

- Based on de Boor's *free* software for 1-D splines.
- Direct product cubic spline fit to $\psi(R, Z)$, which has been output on rectangular grid by DINA or CREATE equilibrium codes.
- Sampling region is rectangle in (ψ, θ)-space.
- Invert 1-D spline fits on lines of constant θ, at equally spaced values of ψ.
- Reject θ values for which $\psi(r)$ is not monotone.

C. de Boor, A practical guide to splines. Springer 1978.

$R(\psi, \theta)$ and $Z(\psi, \theta)$ contours

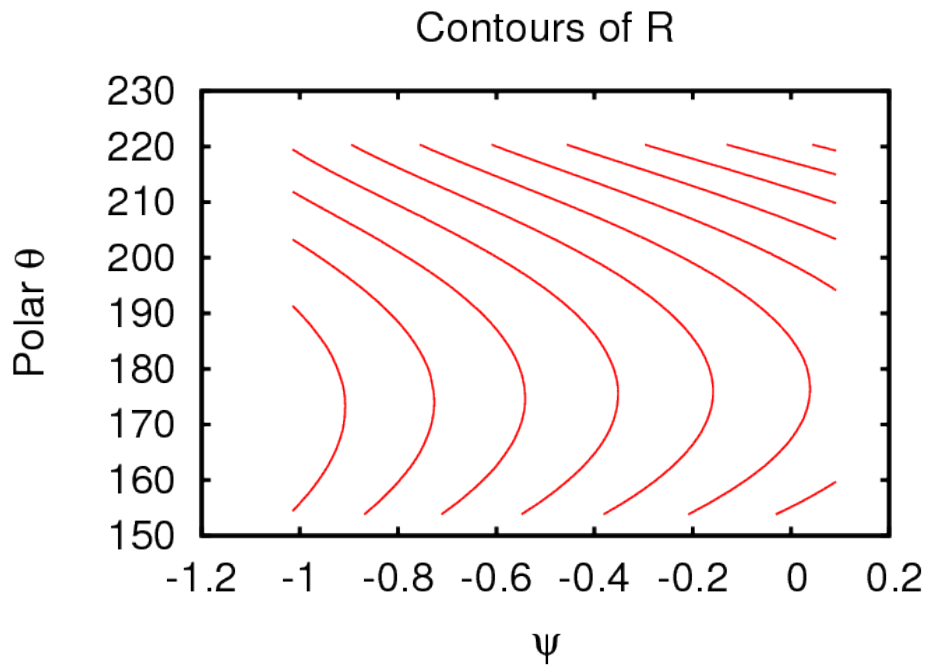

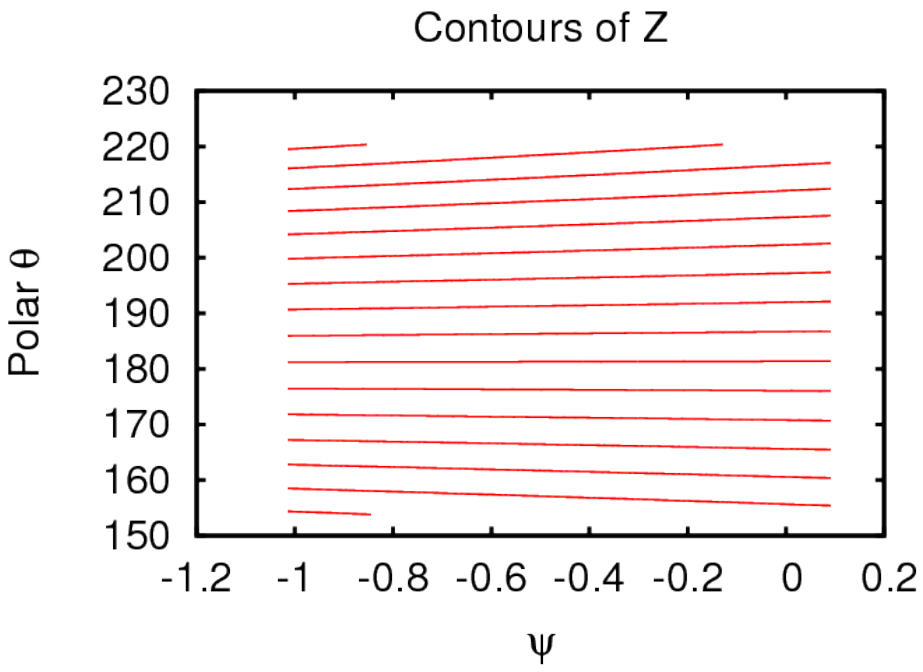

Inverse Map of *Map* is Identity within error of $< 10^{-4}$.

Orientation Plot

- Red coloured semi-panels "shadow" central 'launch' or 'results' geometry.
- Surface triangulation of shadow has 36 146 nodes and 72 260 triangles.
- Power calculations for illustration only.

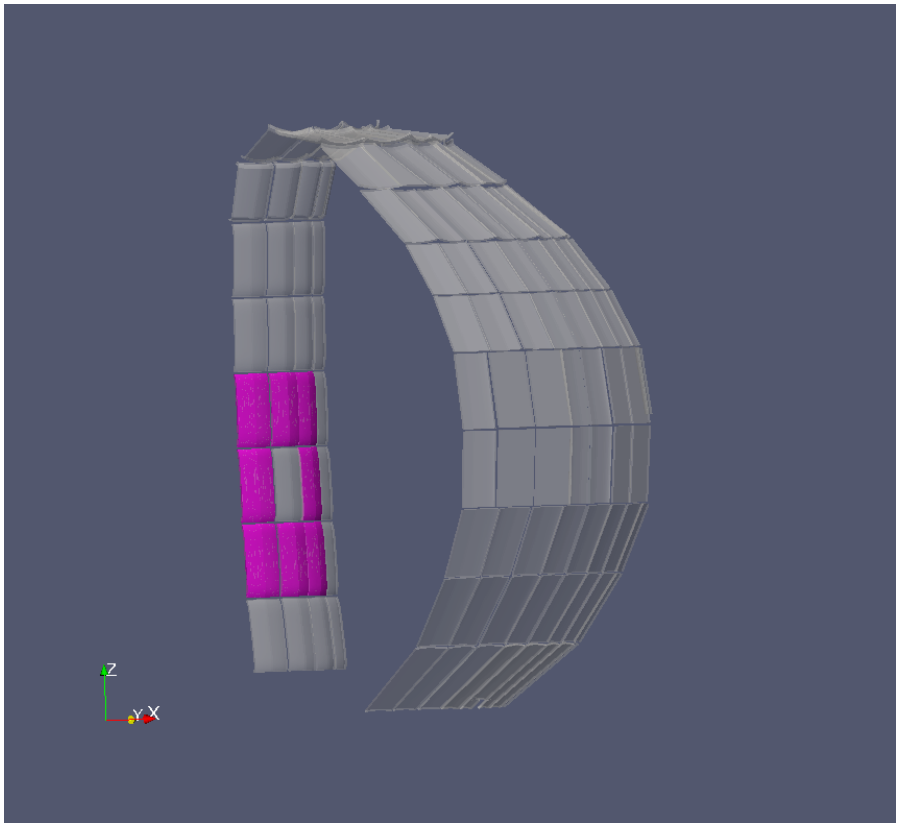

Mesh Refinement Strategy

- Mesh-within-mesh via CADfix FORTRAN API.
- Relatively straightforward additional data structure.
- Symmetric, and triangle shape is preserved.
- Re-use of sample points, but still 3×cost per level of refinement.

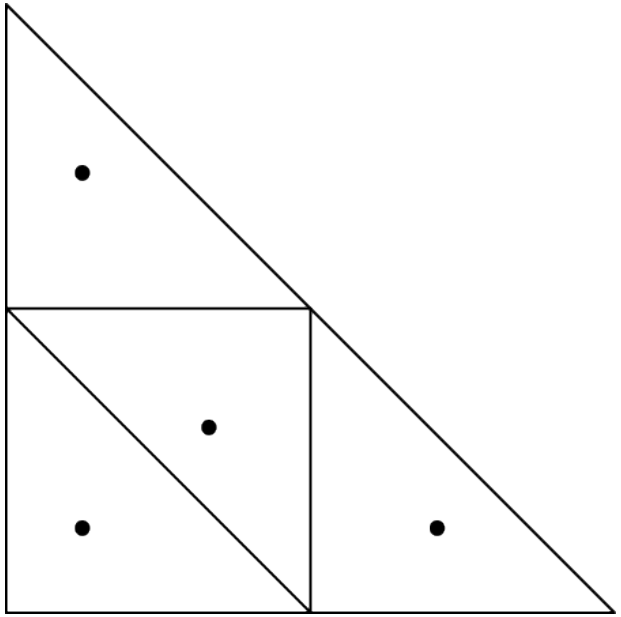

Spots mark barycentres of triangles from which field-lines are launched to check "shadowing" by rest of geometry.

Hierarchical Data Structure

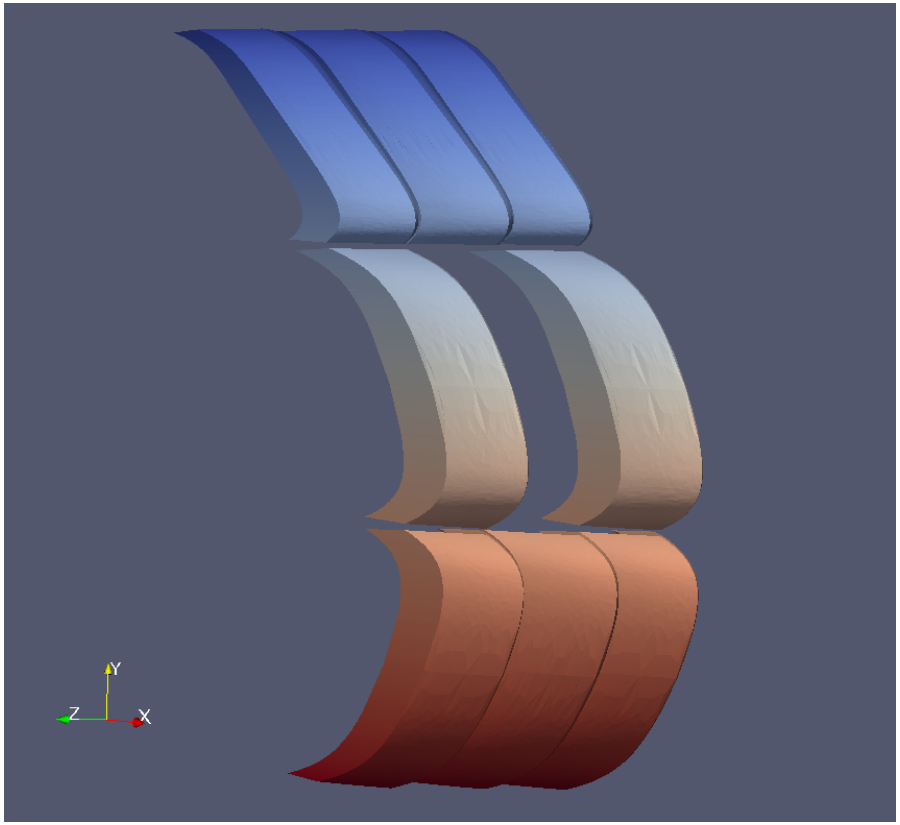

inrshad geometry in (ψ, θ, ζ) coordinates. Red corresponds to larger Z.

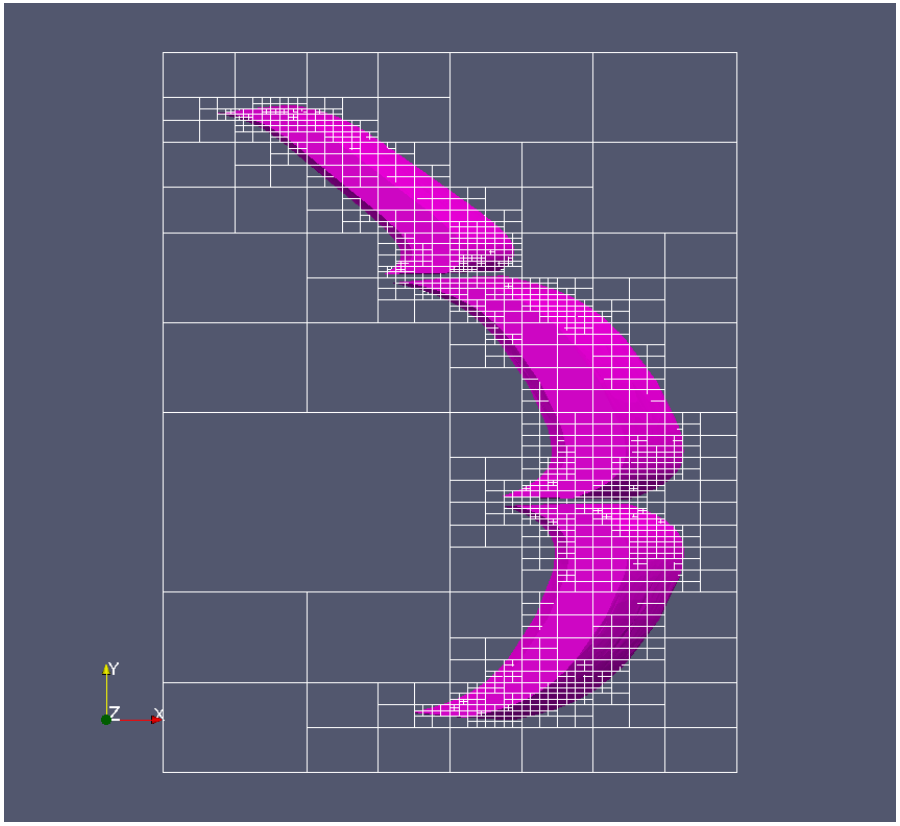

Octree depth of 9, 43 973 leaves.

Base result for Power Density

- Mesh *inres1* shadowed by mesh *inrshad1*.
- 3350 field-lines launched, 382 escape (wetted triangles).
- Total time for calculation 0.77 s (0.21 s for tracking).
- Tracking error control $\epsilon_r = 10^{-6}$; error tested and *as expected*.
- $4 - 11$ points per track.

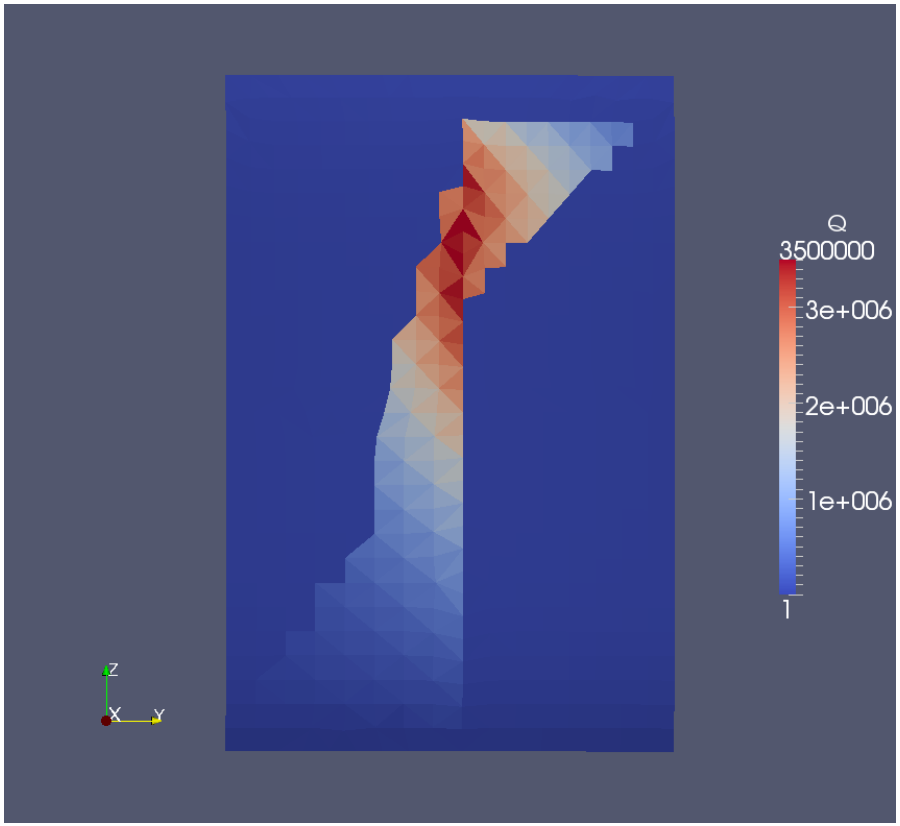

Mesh inres3 shadowed by mesh inrshad2

- 53 600 field-lines launched, 6 050 escape (wetted triangles).
- 289 040 triangles in shadow geometry (potential intersections)
- Total time for calculation 6.95 s (3.73 s for tracking).
- 70 μs/track, cf. 63 μs/track for *inrshad1*

AMD Athlon 64 Dual Core 6000+ 1MB cache, 8GB memory

Effect of Solver Parameters

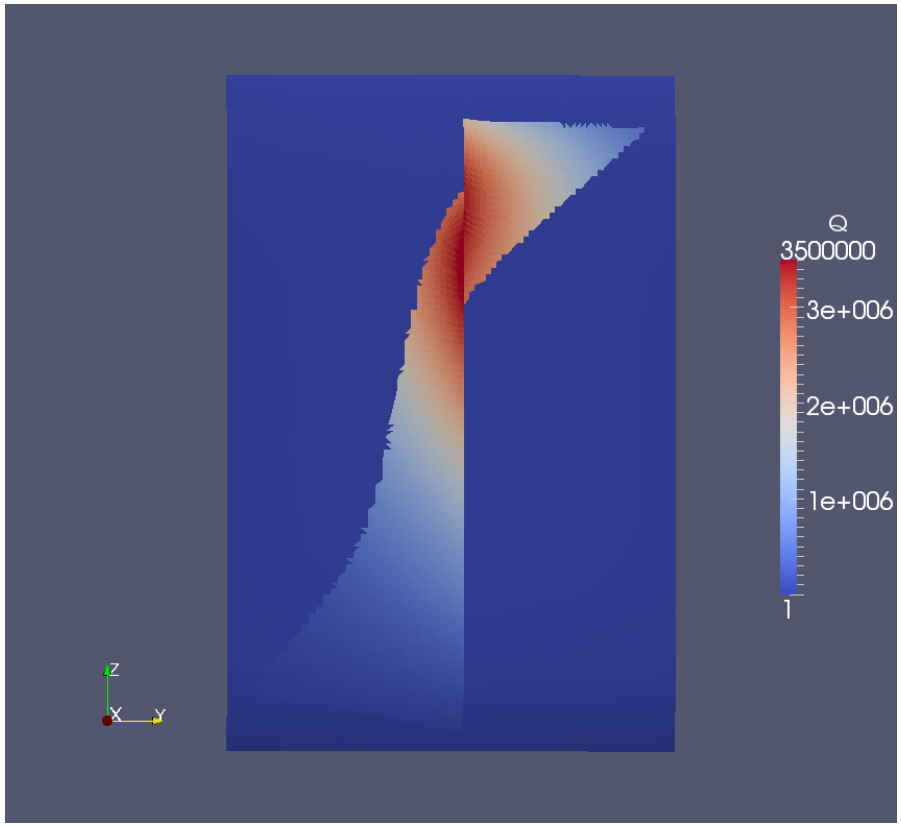

Error control parameter $\epsilon_r = 10^{-6}$

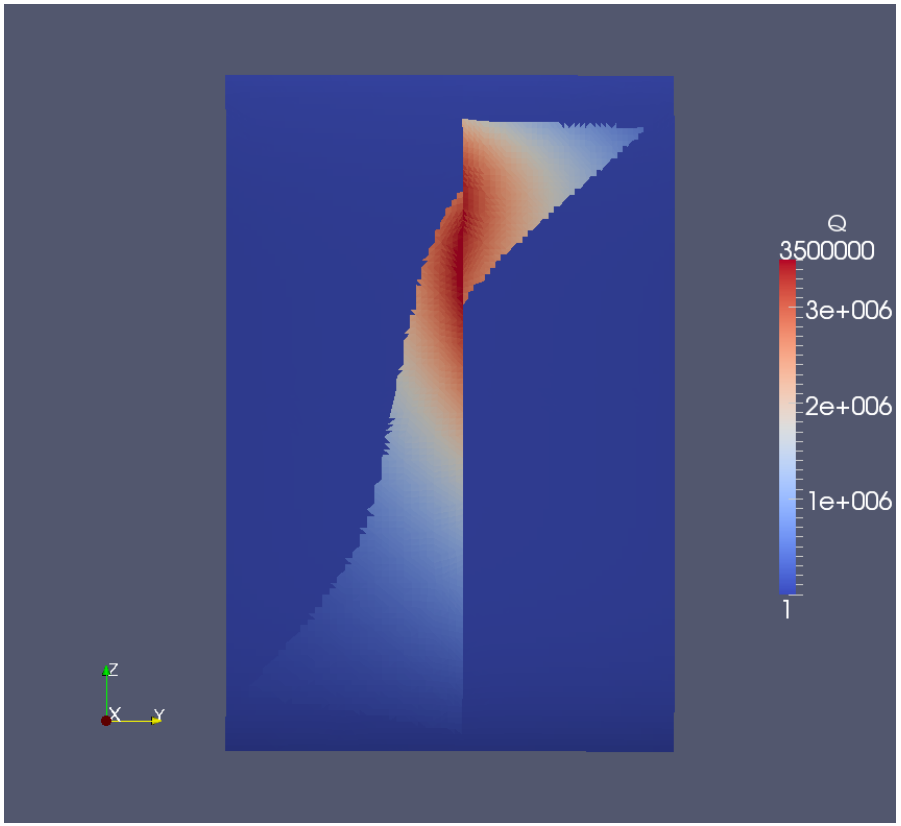

$\epsilon_r = 10^{-4}$

Summary

1. Fast and accurate way of checking power deposition.
2. Software trustworthiness through refinement and visualisation.
3. Time needed scales mainly with number of tracks, *not* so strongly with complexity of geometry.
4. Flexible – SMARDDA also used for charged particle motion in ducts, where over 100× faster than alternative.

King & Arter, ICNSP 2009